



Reticle Purging Approaches by Nitrogen with Enhanced Efficiency

Chen-Wei Ku¹, Shih-Cheng Hu^{1*}, Shean-Hwan Chiou², Po-Shin Lee³

¹ National Taipei University of Technology, Taiwan

² RexChip Electronics Corp., Taiwan

³ Gudeng Precision Industrial Co., LTD, Taiwan

ABSTRACT

The technology roadmap toward smaller structures and thinner layers in semiconductor manufacturing directs attention more and more toward yield-affecting influences from the air quality of manufacturing environment such as water vapor, O₂, CO₂ etc. to absorb high-energy radiation and formation of haze form on reticle surfaces during microlithography processing. A useful method for reducing these yield-affecting influences is purging the reticle surface with nitrogen gas. The main issue is the difficulty in performing purge process in the space between the reticle and pellicle, which has a rather fragile geometry. Our study strives to find the optimized parameters by using computational fluid dynamic (CFD) simulation plus the corresponding inspection results of reticle exposed by 193 nm beam in the fab. Results show that Purging time is sensitive to both the number of purging holes and the purging flow rate. The required purging time can be reduced from 77 seconds to approximately 34 seconds by increasing the purging flow rate from 0.094 L/m to 0.376 L/m (corresponding to purging velocity of 1.0 m/s to 4.0 m/s). However, concerning the breaking of pellicle due to high velocity, the purging velocity was limited to 2.0 m/s (corresponding to its flow rate of 0.188 L/min). By doubling the number of purge/vent holes, with the same flow rate, the required purge time can be even reduced to 33 seconds.

Keywords: Haze defects; Reticle-purging; Computation Fluid Dynamic; 193 nm lithography.

INTRODUCTION

The technology roadmap toward smaller structures and thinner layers in semiconductor manufacturing directs attention more and more toward yield-affecting influences from the air quality of manufacturing environment such as water vapor, O₂, H₂O and CO₂, to absorb high-energy radiation and formation of haze form on reticle surfaces during microlithography processing. The photomask is extremely sensitively to Airborne Molecular Contaminations (AMCs), especially in the 193-nm or 248-nm optical lithography process. Control on AMCs has been the key issue of yield management (Chien *et al.*, 2007; Li *et al.*, 2007). The most noticeable AMCs are water vapor and oxygen. A useful method for reducing AMCs is purging of the photomask box with nitrogen gas (Hu and Tsao 2006; Hu *et al.*, 2007). In the photomask box, the aim of pellicles is to prevent AMCs from falling on the pattern. The exposure process of 193-nm technology can be accomplished in air (Hanet *et al.*, 2005; Kim *et al.*, 2006; Gordon *et al.*, 2007). Therefore, purging nitrogen gas to

the pellicle space for contamination control is essential to avoid image degradation and to accomplish the exposure. The main issue is the difficulty in performing purification in the space between the reticle and pellicle, which has a rather fragile geometry (Bunner *et al.*, 1983; Cotteet *al.*, 2002; Abdo *et al.*, 2003; Meixneret *al.*, 2004). The current technology for fabricating pellicle frames is based on anodized aluminum. While there are general specifications on dimensions and surfaces, lots of attention has been directed to detailed requirements mainly because that the demands on the pellicle frame are not rigorous (Johnstone *et al.*, 2003). However, as the optical lithography wavelength grows shorter, issues previously neglected may turn out to be major shortcomings (McClay and McIntyre *et al.*, 1999). Exposure tool manufacturers are using a nitrogen purification system to decontaminate the optical lithography in systems (Okada *et al.*, 1998; Liberman *et al.*, 1999; Cottea *et al.*, 2004). For example, the broadly adopted approach of purging the pellicle space through a pellicle film is now considered to be both difficult and problematic in leaving open the possibility of pellicle film rupture due to pressure difference across the pellicle film. Moreover, this approach can no longer accomplish sufficient purging to meet the growingly sophisticated needs. An improved approach that has been discussed in the industry is to perforate a number of small purging holes (inlets) and vent holes (outlets) in the pellicle frame,

* Corresponding author. Tel.: +886-2-2771-2171 ext. 3512;
Fax: 886-2-2731-4919
E-mail address: f10870@ntut.edu.tw

as shown in Fig. 1. While the frame dimensions vary with the manufacturers and types of pellicles. The broadly adopted dimension of the holes on the four sides is 1.0 mm in diameter. A transparent pellicle is placed on the surface of a reticle to protect its surface from contamination. During certain conditions, crystals formation of haze forming on reticle surfaces, the sulfate ion (SO_4^{2-}) left on the mask surface after SPM (scanning probe microscopes) step is known as the most important source resulting in the formation of haze defects. And ammonium sulfate has been known to be mostly responsible for haze defects formation on the mask surface. Recent investigation reveals that the other chemicals such as hydrocarbons, Na, F, Mg, K, Cl or Al are also the results of haze defects. A major problem in the integrated circuit (IC) industry is that the manufacturing process may experience malfunction due to haze contamination on the mask once the reticle has been exposed to ArF radiation. In addition to the previously mentioned shortcomings, the traditional way of purging works by supplying N_2 into reticle SMIF-Pod to help clean air slowly diffuse into the space between the reticle and the pellicle. However, the purging time is in need of improvement. The new approach proposed in this study seeks to avoid these issues by developing a prototype purge station to supply the nitrogen into the pellicle frame directly.

Our study further strives to find the optimized parameters by using computational fluid dynamic (CFD) simulation. The purging process should be performed right before the reticle is going to be exposed and repeated after the reticle is exposed so as to effectively reduce the generation of haze. Ultimately, this study aims to enhance the performance of purging process by identifying the optimal parameters such as number and position of purging holes and purging flow rate using computational fluid dynamic (CFD) simulation.

RESEARCH METHODS

Model Equations

The CFD study was performed using a commercial FLUENT software (version 6.3 (2007)), which has been successfully applied to solve various types of turbulent flows. The physical dimension for a typical purge condition (with 4 vent holes) is shown in Fig. 1.

The mixing and transport of various species were modeled by solving conservation equations, which describe convection, diffusion, and reaction sources for each component species. When solving conservation equations for species. The conservation equation takes the following general form:

$$\frac{\partial}{\partial t}(\rho Y_i) + \nabla \cdot \left(\rho \vec{v} Y_i \right) = -\nabla \cdot \vec{J}_i + S_i \quad (1)$$

Where Y_i is solution of a convection-diffusion equation for the i th species and ρ is fluid density. S_i is the rate of creation by addition from the dispersed phase plus any

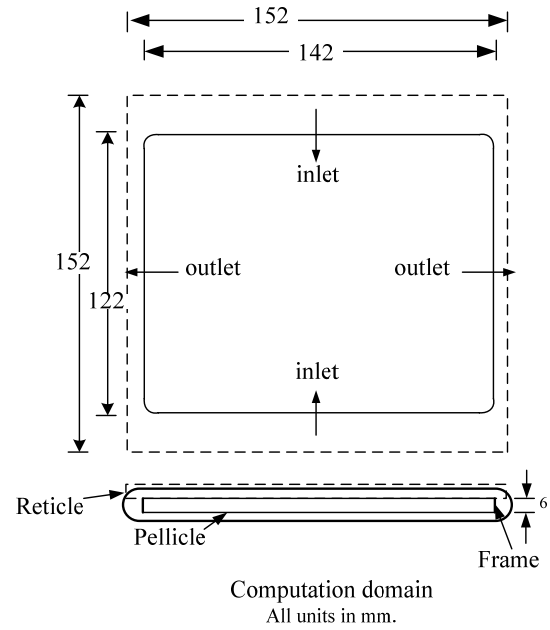


Fig. 1. The physical dimension for a typical purge condition.

user-defined sources. An equation of this form will be solved for $N-1$ species where N is the total number of fluid species present in the system. Since the mass fraction of the species must sum to unity, the N th mass fraction is determined as one minus the sum of the $N-1$ solved mass fractions. In this study, we solve a species mixing problem without reactions. The species transport equation for the k' th species is in the following general form:

$$\frac{\partial}{\partial t}(\rho c_k) + \frac{\partial}{\partial x_i}(\rho u_i c_k) = \frac{\partial}{\partial x_i}(\Gamma_{c_k} \frac{\partial c_k}{\partial x_i} - \overline{\rho u'_i c'_k}) + S_{c_k} \quad (2)$$

$k = 1, \dots, N$

Where N and S_{c_k} are the number of species and source term supplied for equations, and the species Γ_ϕ is the effective exchange coefficient for the dependent variable. The differential equation given by Eq. (2) is integrated with respect to momentum using a second-order upwind scheme. The mass diffusion was given in the following form:

$$\vec{J}_i = - \left(\rho D_{i,m} + \frac{\mu_t}{S_{ct}} \right) \nabla Y_i \quad (3)$$

where S_{ct} is the turbulent Schmidt number ($\mu_t / \rho D_t$, where μ_t is the turbulent viscosity and D_t is the turbulent diffusivity) is assumed to be 0.7. Three species i.e. nitrogen, oxygen and air were considered. The purging experiment is a complex transient process, due to the tiny thickness (about $\sim 1 \mu\text{m}$) of the pellicle, and the relatively high diffusion coefficients of gases in the rubbery pellicle material, transient kinetics associated with establishing concentration within the pellicle film can be neglected to a first approximation.

Boundary Conditions and Grid Independence Test

Prescribed value and Neumann boundary condition were applied to the inlet and outlet, respectively. No-flux boundary condition and standard wall function were imposed in all boundary walls. These are conventional boundary conditions. The pellicle film was assumed to be a porous media that uses an addition of momentum source. The source term is composed of two parts: a viscous loss term, and an inertial loss term.

$$S_i = -\left(\frac{\mu}{\alpha} v_i + C_2 \frac{1}{2} |v| v_i\right) \quad (4)$$

where S_i is the source term for the i th (x , y , or z) momentum equation, $|v|$ is the magnitude of the velocity, α is the permeability, and C_2 is the inertial resistance factor. Table 1 shows the boundary conditions in this study.

Grid testing for both space and time domain were performed. The final grid number and time step adopted were 199,474 and 1 second, respectively. Maximum and minimum cell sizes were $5.79 \times 10^{-12} \text{ m}^3$ and $1.57 \times 10^{-9} \text{ m}^3$, respectively.

Cases Description

The reticle-purging process must be accomplished as quickly as possible without breaking the pellicle. Major factors affecting reticle purging are all related to boundary conditions, including the purging gases, the purging velocity (flow rate), the number of purging/vent holes. Table 2 tabulates the detail of the three simulation cases. The purge flow rate ranges from 0.094 L/min to 0.376 L/min, corresponding to its purge velocity of 1.0 m/s to 4.0 m/s in case 1. In case 1, inlets were located in the long sides while outlets were in short sides. Conversely, inlets were located in the shorter sides while outlets were in long sides in case 2. The number of purge/vent holes were doubled i.e. four purge holes and four vent holes in case 3.

The purge process was regarded to complete when two factors were arrived, i.e. 500 ppm of oxygen content and 1% of relative humidity.

RESULTS AND DISCUSSION

Effect of Purge Gas

Two different kind of purge gases i.e. nitrogen and compressed dry air was investigated on their influence on the removal of water vapor content. It was found that using the compressed dry air results slightly difference in purge efficiency from using nitrogen gas (see Fig. 2). This is because there is only minor difference in the diffusivity between the compressed dry air and nitrogen gas. However, it should be noted that if oxygen is the AMCs to be controlled, the compressed dry air can not be a purge gas.

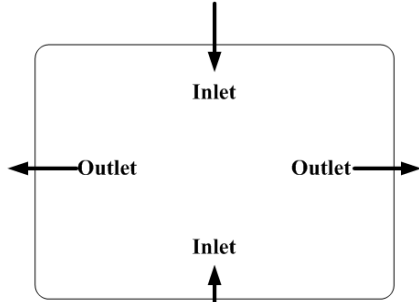
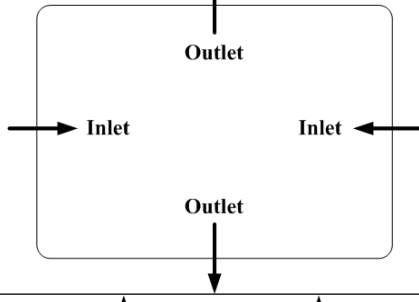
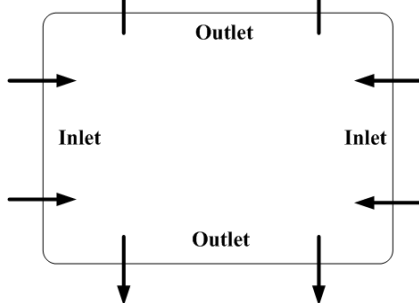
Effect of Vent Hole (Outlet)

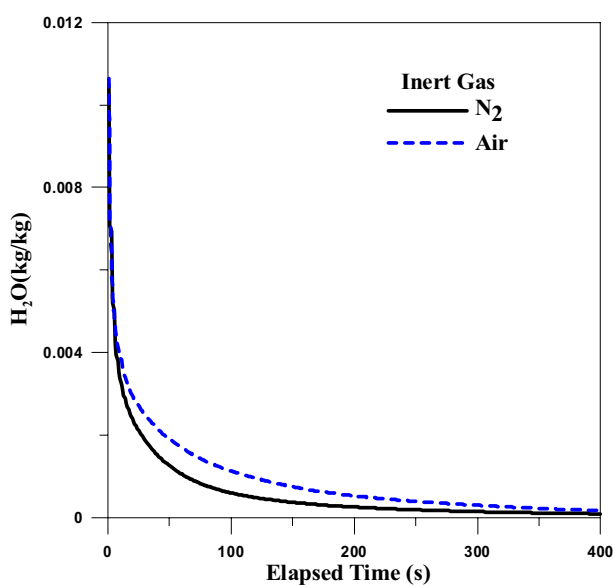
Figs. 3(a) and 3(b) show the nitrogen distribution on the reticle surface with one vent hole and with two vent holes after 30 seconds with the traditional way of purging works by supplying nitrogen into reticle SMIF-Pod to diffuse the nitrogen into the space between the reticle and the pellicle. Both figures show that the overall gas diffusion on the edge of pellicle frame is less than the one in the center and this might result in the accumulation of contaminant on the edge and cause the formation of haze. Fig. 3(b) exhibits a more uniform distribution and a higher concentration of nitrogen gas, which relates to a lower risk of defect. This was confirmed by inspection results of reticle exposed by 193 nm laser beam in the fab, as shown in Figs. 4(a) and 4(b). In Fig. 4(a), with one vent hole, significant haze formations (indicated by red triangle symbols) were detected on the edge of pellicle frame than those in Fig. 4(b). In the fab, the purging process was operating inside the chamber, and the pressure variation in the chamber was in range of 40kPa–80kPa.

Table 1. Boundary conditions.

(1) Velocity Inlet	$U = U_{\text{purge}}$, $C = C_0$, turbulent intensity = 10 (%), $D_h = 0.00032 \text{ (m)}$ U_{purge} : purging velocity (m/s) C_0 : Species Mass Fractions (Nitrogen = 99.999%) D_h : Hydraulic Diameter(m)
(2) Pressure Outlet	$P_{\text{outlet}} = P_f$, $P_f = 1/2(P_c + P_e)$, P_c is the interior cell pressure neighboring the exit face f , P_e is the specified exit pressure
(3) Wall Surface	No slip condition on the wall surface $(u = v = w = 0)$, and $\frac{\partial k}{\partial n} = \frac{\partial \varepsilon}{\partial n} = \frac{\partial C}{\partial n} = 0$ u, v, w : velocity components k : turbulence kinetic energy ε : dissipation rate of the turbulence kinetic energy C : species
(4) porous zone	$S_i = -\left(\frac{\mu}{\alpha} v_i + C_2 \frac{1}{2} v v_i\right)$, $\alpha = 10^{13} \text{ scc.cm/cm}^2 \cdot \text{s.Pa}$, permeability of a soft pellicle film, $C_2 = 9 \times 10^7$, inertial resistance factor

Table 2. The three simulation cases (a purging hole is an inlet and a vent hole is an outlet).

Cases	Arrangement of purging holes and vent holes	Purge (inlet) velocity (m/s)
1		1.0, 2.0, 3.0 or 4.0
2		1.0, 2.0, 3.0 or 4.0
3		0.5 or 1.0

**Fig. 2.** Predicted volume averaged concentration of water vapor content vs. elapsed time for different purge gases i.e. nitrogen and compressed dry air.

Effect of the Arrangement of Purge Holes (Inlets) and Vent Holes (Outlets)

Figs. 4(a), 4(b) and 4(c) show the flow patterns on the reticle surface in case 1, case 2 and case 3, respectively. In cases 1 and 2, two large recirculation zones were noticed in the inlet region. The recirculation zones in case 1 occupy a larger area than those in case 2, causing an increase in the purging time. The other concern is the vertical velocity on the retical surface. A high vertical velocity means a high risk of breaking of the pellicle due to the inlet purge gas. In case 1, the magnitude of vertical velocities were 0.09 m/s, 0.13 m/s, 0.17 m/s and 0.23 m/s for inlet velocities of 1.0 m/s, 2.0 m/s, 3.0 m/s and 4.0 m/s, respectively. Concerning the breaking of pellicle due to high vertical velocity on the pellicle surface, the purge velocity was limited to 2.0 m/s (corresponding to its purging flow rate of 0.188 L/min). The number of purge/vent holes were doubled i.e. four purge holes and four vent holes in case 3. Fig. 5(c) shows small recirculation areas, eliminating the residual air in the corner area of the pellicle, which is the most difficult place that nitrogen can reach. The depletion time history of

oxygen concentration at the outlet in case 3 was also lower than in cases 1 and 2.

Fig. 6 presents the predicted volume averaged concentration of oxygen concentration vs. elapsed time in all cases. The oxygen concentration decreases dramatically in the first 20 seconds for all cases. It is observed that in

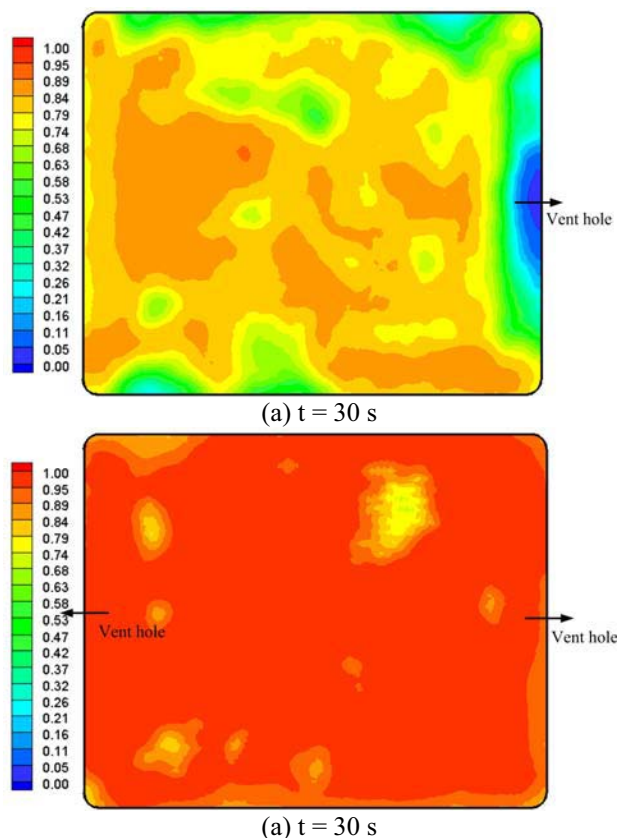
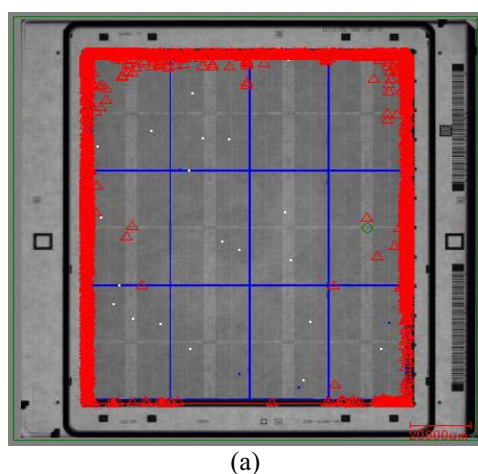
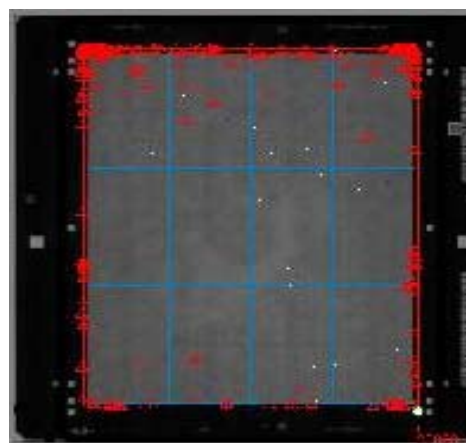


Fig. 3. (a) Predicted nitrogen distribution on the reticle surface with one vent hole, (b) Predicted nitrogen distribution on the reticle surface with two vent hole.



(a)

Fig. 4. (a) Measured photoinduced defects detected for reticle pellicularized with 193 nm with one vent hole, (b) Measured photoinduced defects detected for reticle pellicularized with 193 nm with two vent holes.



(b)

Fig. 4. (continued).

purge velocity from 1 m/s to 4 m/s. When purge velocity was 2 m/s, the purging efficiency of case 2 was comparable when to the case 1 with purge velocity of 3.0 m/s. As the number of purge holes increases in case 3, the resistance of the purging flow injected into the pellicle volume decreases for a given time period. Consequently, a reduction in the total purging time was achieved. For case case 1 the required purge time can be reduced from 77 seconds to approximately 34 seconds by increasing the 3, when purge velocity was 0.5 m/s (purging flow rate of 0.094 L/s), the required purge time was 68 seconds. For the cases 1 and 2 with the same purge flow rate (purging velocity of 1.0 m/s), the required purge time were 80 seconds and 92 seconds, respectively. The required purge time can be even reduced to 33 seconds with purging velocity of 1.0 m/s (purging flow rate of 0.188 L/s) in case 3.

CONCLUSION

Based on the results and discussion, the following conclusions are drawn:

1. No significant difference on purge efficiency for oxygen removal by using either nitrogen or compressed dry air. However, for removal of oxygen compressed dry air should not be used.
2. Locating the purging holes in the short sides and vent holes in the short sides of the frame (case 2) is a better arrangement in terms of purging efficiency than those locating the purging holes in the long sides and vent holes in the short sides of the frame (case 1).
3. Numerical study and photo-inspection in the fab confirm that, with the same purging flow rate, purges with two purging holes can create a more uniform nitrogen purge than that with one purging hole, especially in the edge of pellicle frame where haze formation often happens.
4. Purging time is sensitive to both the number of purging holes and the purging flow rate. The required approximately 34 seconds by increasing the purging flow rate from 0.094 L/m to 0.376 L/m (corresponding

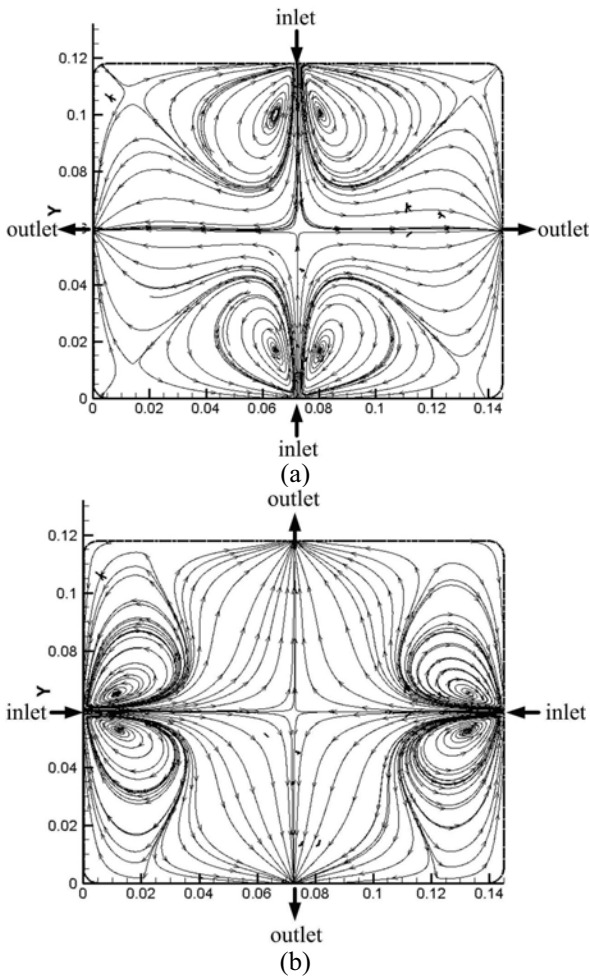


Fig. 5. (continued).

Fig. 5. Predicted streamline patterns on x-y plane of the pellicle surface in case 1 (a), case 2 (b) and case 3 (c).

to its purging velocity of 1.0 m/s to 4.0 m/s). However, concerning the breaking of pellicle due to high velocity, the purging velocity was limited to 2.0 m/s (corresponding to its flow rate of 0.188 L/min). By doubling the number of purge/vent holes, with the same flow rate, the required purge time can be even reduced to 33 seconds.

- The future works of this study include using diffuser as a purging inlet to improve the purging efficiency and taking into account the water vapor absorption/desorption property of the frame material, purging time can be reduced from 77 seconds to which has significant influence on water vapor content in the final purge state (Hu and Tsao, 2006; Hu et al., 2007).

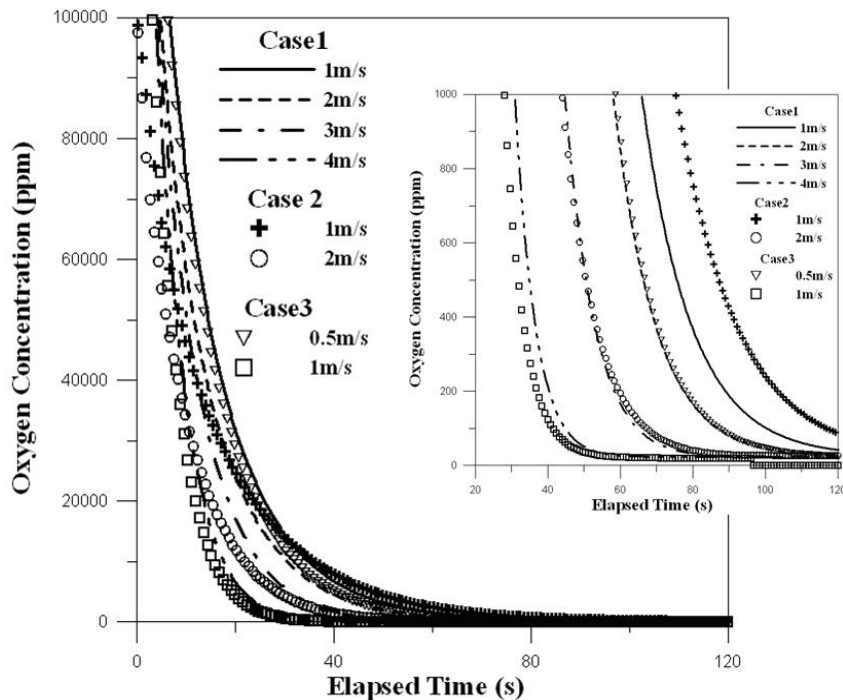


Fig. 6. Predicted volume averaged concentration of oxygen concentration vs. elapsed time in all cases.

ACKNOWLEDGMENTS

This research was supported by RexChip Electronics Corp. and funded by Gudeng Precision Industrial Co. Ltd. The authors gratefully acknowledge the generous support and valuable suggestions from our colleagues at Center for Cleaning Technology Research, National Taipei University of Technology.

REFERENCES

- Abdo, A.Y., Nellis, G.F., Diab, A.K., Cotte, E.P. and Chalekian, A.J. (2003). Experimental Investigation of Hard Pellicle Purge Processes. *Proc. SPIE*. 5256: 897-904.
- Bunner, T.A., Ausschnitt, C.P., Dully, D.L. (1983). Pellicle Mask Protection for 1:1 Projection Lithography. *Solid State Technol.* 26: 135-143.
- Chien, C.L., Tsai, C.J., Ku, K.W. and Li, S.N. (2007). Ventilation Control of Air Pollutant during Preventive Maintenance of a Metal Etcher in Semiconductor Industry. *Aerosol Air Qual. Res.* 7: 469-488
- Cotte, E.P., Reu, P.L. and Engeistad, R.L. (2002). Experimental and Numerical Studies of the Response of Photomask Hard Pellicles to Acoustic Excitation. *Proc. SPIE*. 4889: 1121-1132.
- Cottea, E., Häblerb, R., Utessa, B. and Antesbergera, G. (2004) Pellicle Choice for 193-nm Immersion Lithography Photomasks. *Proc. SPIE*. 5567: 511-520.
- Fluent 6.3 User's Guide (2007). Fluent Inc., Lebanon, U.S.A.
- Gordon, J.L. Frisa, E.C., Chovino, M., Chan, D.Y., Keagy, J. and Weins, C. (2007). Influence of Environmental Components on Haze Growth. *Proc. SPIE*. 6607: 660707.
- Han, S.J., Kim, B.H., Park, J.H., Kim, Y.H., Choi, S.W. and Han, W.S. (2005). The Study on Causes and Control Methods of Haze Contamination. *Proc. SPIE*. 5645: 109-113.
- Hu, S.C. and Tsao, J.M. (2006). Purge of a Front Opening Unified Pod (FOUP) with Nitrogen for 300 mm Wafer Manufacturing, *Jpn. J. Appl. Phys.* 42: 5269-5271.
- Hu, S.C., Wu, T.M. and Lin, H.C. (2007). Design and Evaluation of a Nitrogen Purge System for the Front Opening Unified Pod (FOUP). *Appl. Therm. Eng.* 27: 1386-1393.
- Johnstone, E., Dieu, L., Chovino, C. and Reyes, J. (2003). 193-nm Haze Contamination: A Close Relationship between Mask and Its Environment. *Proc. SPIE*. 5256: 440.
- Kim, S.J., Kyoung, J.S., Park, J.B., Kim, Y.H., Park, S.W., An, I.S. and Oh, H.K. (2006). The Influence of Transmission Reduction by Mask Haze Formation in ArF Lithography. *J. Korean Phys. Soc.* 49: 518-523.
- Li, S.N., Shih, H.Y., Yen, S.Y. and Yang, J. (2007). Case Study of Micro-Contamination Control. *Aerosol Air Qual. Res.* 7: 432-442.
- Liberman, V., Bloomstein, T.M., Rothschild, M., Sedlacek, J.H.C., Uttaro, R.S., Bates, A.K., Van Peski, C. and Orvek, K. (1999). Materials Issues for Optical Components and Photomasks in 157 nm Lithography. *J. Vac. Sci. Technol. B*. 17: 3273-3279.
- McClay, J.A. and McIntyre, A.S.L. (1999). 157nm Optical Lithography: The Accomplishments and the Challenges. *Solid State Technol.* 42: 57.
- Meixner, D.L., Ganguli, R., Robinson, T., Jeng, D.Y., Morris, M.W. and Chaudhuri, S. (2004). Porous Silica Frame for Deep Ultraviolet Lithography. *Proc. SPIE*. 5040: 1018-1024.
- Okada, I., Saitoh, Y., Deguchi, K., Fukuda, M., Ban, H. and Matsuda, T. (1998). Mask Contamination Induced by X-Ray Exposure. *Jpn. J. Appl. Phys., Part 1*. 37: 6808-6812.
- Zell, T. (2006). Present and Future of 193 nm Lithography. *Microelectron. Eng.* 83: 624-633.

Received for review, January 8, 2009

Accepted, July 10, 2009